Data assimilation for urban noise mapping with a meta-model

Antoine Lesieur, Vivien Mallet, Pierre Aumond, Arnaud Can

Version of Record: https://www.sciencedirect.com/science/article/pii/S0003682X21000311
Manuscript_af22619284c8bff8a47a848f9485b418

Data assimilation for urban noise mapping with a meta-model

Antoine LESIEUR, Vivien MALLET, Pierre AUMOND, Arnaud CAN

Abstract

Accurately predicting dynamic noise levels in urban environments is non-trivial. This study aims to optimally combine both simulated and empirical data. Acoustic data from microphone arrays, traffic and weather data was merged with a simulated noise map, created with a statistical emulator tool (meta-model). Each hour, a noise map is generated by the meta-model with the measured traffic and weather data. This map is algorithmically merged with the measured readings to form a new composite map. The resulting analyzed map is the best linear unbiased estimator under certain assumptions. The performance is evaluated with leave-one-out cross-validation. The performance of the method depends on the accuracy of the meta-model, the input parameters of the meta-model and the structure of the error covariances between the simulated noise level errors. With 16 microphones over an area of 3 km^2, this new method achieves a reduction of 30 % of the root-mean-square error when compared to a meta-model only.

1. Introduction

A regulatory noise map is a representation of the equivalent average noise level field over an urban area. These maps are useful to evaluate scenarios for predictive applications, and are produced by many cities around the world. Within Europe, every agglomeration with more than 100 000 inhabitants is required to produce a noise map every 5 years. The standard reference for producing noise maps in the EU is CNOSSOS-EU (Kephalopoulos et al., 2012), it is currently applied following the directive 2015/996 (European Commission, 2015).

Most urban scale noise maps use models similar to CNOSSOS-EU. They proceed as follows, first, the emission algorithm is based on a discretization of the road. Each road section is described by a set of point sources whose

intensities depend on the road, traffic (flow rate and speed) and weather data. Secondly, the propagation algorithm determines the sound attenuation between each point source and each receiver based on geometry and weather data, after a ray path calculation. When this method is applied at a city scale, the high number of sources and receivers makes this method computationally expensive. It is not adapted to the generation of hourly or even daily noise maps: the computation time would be too high. This approach is limited by the quality of the input data used to generate the noise map. Traffic data may only be measured on a subset of roads, which may not provide an accurate representation of wider situation.

Observation-based approaches have been developed to build maps solely from noise measurements. (Wei et al., 2016) built an interpolating model based on observations and a method to propagate the observed sound level. (Aumond et al., 2018) statistically interpolated noise measurements with a kriging approach; this approach gave satisfactory results in the vicinity of the measurement devices but suffered from the lack of sensors when estimating the noise level over a wider range.

Several attempts have been made to enrich noise maps with observational data. (Ventura et al., 2018) assimilated observations from mobile phone microphones in order to improve a pre-calculated noise map. However this process is useful only when a large number of mobile observations can be collected for this task. The DYNAMAP project (Zambon et al., 2016) updates noise maps by scaling the noise levels of pre-calculated noise maps using the differences observed between measured and calculated original grid data for different classes of roads. (De Coensel et al., 2015) speculated about combining a noise mapping model with mobile noise measurements to increase the resolution of the noise map and fixed measurements to allow a dynamic noise mapping. These methods however purely rely on statistical methods (Least Mean Squares) and do not take into account either error propagation or traffic dynamics models. (Eerden et al., 2014) finally infers the noise mapping software inputs from noise observation by estimating the emission sources from the observed noise measures in the vicinity of the roads. This method uses a forecasting sequential approach rather than a spatial approach.

The approach proposed in this paper offers (1) to use a dynamic noise mapping, quickly generated by a meta-model (also called surrogate model) and based on real-time weather and traffic input data, and (2) to spatially enrich the noise map with noise observation data thanks to a data assimilation process which includes a simulation error model.

The objective of this paper is to develop a strategy to display accurate hourly noise maps, starting with:

- An open source noise mapping software,
- Annually averaged input data for the simulation,
- Hourly traffic and weather data from local sensors,
- A network of microphones spread across the study area.

The approach presented in this paper uses both meta-model outputs and observational data to allow a dynamic approach where 1-hour noise levels can be evaluated. This provides a view on the city noise dynamics and a finer analysis of the exposure to noise, at night and during peak hours and it is very fast to compute. This paper proposes a three-step approach:

1. Meta-modeling: the noise map produced by a classical noise model is quickly approximated using a meta-model. A meta-model is a replacement for a noise model when only a limited number of selected input parameters are allowed to change. The meta-model is trained with a sample of simulated noise maps, from which it is possible to statistically represent the relation between the selected input parameters and the corresponding noise maps.
2. Data assimilation design: the simulation error covariance matrix is computed with some training observations.
3. Data assimilation process: the simulation is corrected anywhere in space by the observation data.

A performance evaluation step will be executed with a leave-one-out cross validation method.

This paper explains in section 2 the framework where the study lies (section 2.1), the software and data used for the study (sections 2.2 and 2.3), how the meta-model is built (section 2.4), how the data assimilation process works (section 2.5) and the method conducted to validate the process (section 2.6). In section 3, the performance of the data assimilation is evaluated.

2. Methods

2.1. Description of the framework

The proposed approach consists in relying on a metamodel which reproduces the outputs of a reference software in a very short computing time,

and hourly traffic and acoustic data, to produce hourly noise maps. This approach is inspired by a study done for air quality simulation (Tilloy et al., 2013). All the steps of the data assimilation process are summarized in figure 1.

The approach has three steps:

- Build a meta-model from reference simulations (section 2.4);
- Build a gain matrix $\mathbf{K}$ used in the data assimilation algorithm (Appendix);
- Build a data assimilation algorithm which corrects the results based on a error covariance matrix (section 2.5).

2.2. Reference noise mapping software

2.2.1. Presentation

The simulator used in this study is NoiseModelling v3.0 (Bocher et al., 2019), an open source software designed to produce noise maps for evaluating the noise impact on urban mobility plans. Its input are traffic data, topographic data (buildings distribution, altitude, surface types, ...) and meteorological data (temperature, hygrometry, probability of occurrence of favorable atmospheric conditions ...). The version used in this paper is especially designed to run multiple simulations (Aumond et al., 2020). A first call to the simulator computes a matrix of rays between the source/receiver pairs, which is the longest step for a noise mapping software. Each call to the reference noise mapping software with a new set of parameters is then much faster since it only requires to compute the attenuation along each pre-computed path.

The input traffic data along each road is discretized into a set of point noise sources, an emission value is assigned which depends on the speed, the flow rate and other traffic parameters (type of road, type of vehicle, ...). The output noise level field is represented by a regular grid of receivers. NoiseModelling uses a path finding method similar to the one proposed by CNOSSOS-EU which computes the path taken by the acoustic waves between the sources and the receivers, taking into account the propagation distance, the number of reflections and whether the diffractions are taken into account or not. The software then computes the attenuation along each path for a selected range of octave bands (63 Hz, 125 Hz, 250 Hz, 500 Hz, 1 kHz, 2 kHz,

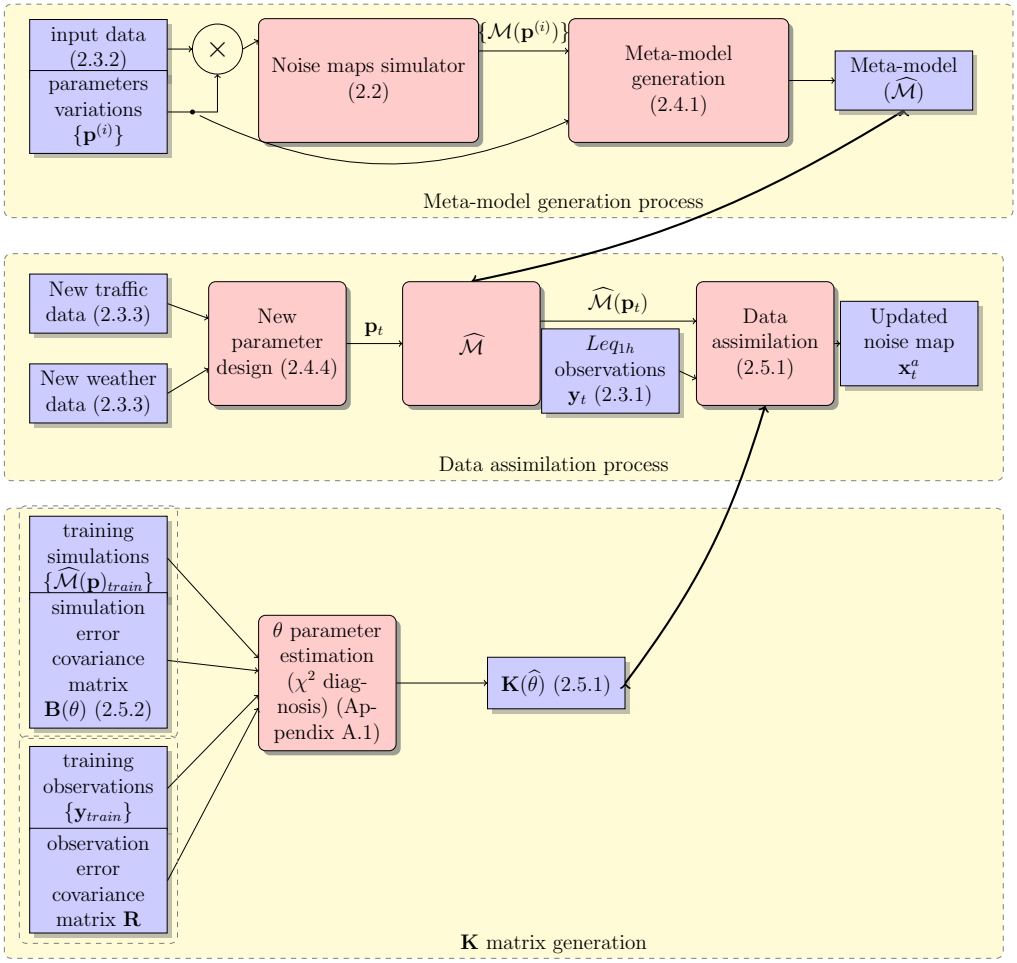

Figure 1: Functional diagram of the data assimilation process.

4 kHz and 8 kHz) in accordance with the CNOSSOS-EU method. The sound level at a receiver is the sum of the contributions of each source. The final output is a grid of receivers with an attributed sound level value computed in dB(A).

2.2.2. Characteristics of the simulation

The simulated area is an area located in the 13$^{\text{th}}$ district of Paris, France. Its surface is about 3 km^2. The receivers, where noise levels will be calculated, are located on a regular grid of step $\Delta x = 15$ m. Receivers have also been located at the location of the observation points. The total number of receivers is $n = 8456$. All these receivers are positioned at a fixed height of 4 m. Note that the actual height of the microphones does not always match the height of the simulation. The only available value for the height of the microphone is the floor level where they were positioned, which is too vague to be precisely set as an input value. The propagation parameters are: 250 m for the propagation distance, 100 m for the distance after reflexion, one order of reflection and one order of diffraction.

2.2.3. Standard noise map using annually averaged data

The nominal L_{day} field distribution given by the reference noise mapping software with this input data is shown in figure 2. The nominal $L_{evening}$ and L_{night} have also been computed in the study.

2.3. Observation data

2.3.1. Noise data

This study uses data collected in the 13$^{\text{th}}$ district of Paris, France during a measurement campaign conducted in 2015 by Lavandier et al. (2016). A network of 25 microphones has been deployed across the study area. 16 of them have been selected for the present study, the ones that had simultaneously an exploitable set of data during the entire time period. They have recorded the noise level L_{f_i} in dB for every one-third octave f_i from 63 Hz to 20 kHz with a time step of $\Delta t = 125$ ms, from January 1, 2015 to September 30, 2015. The indicator used in this study is $LAeq_{1h}$

The spatial distribution of the sensors is shown in figure 3.

2.3.2. Annually averaged input data

The input files of the reference noise mapping software are the buildings distribution and the annually averaged road traffic map during the daytime

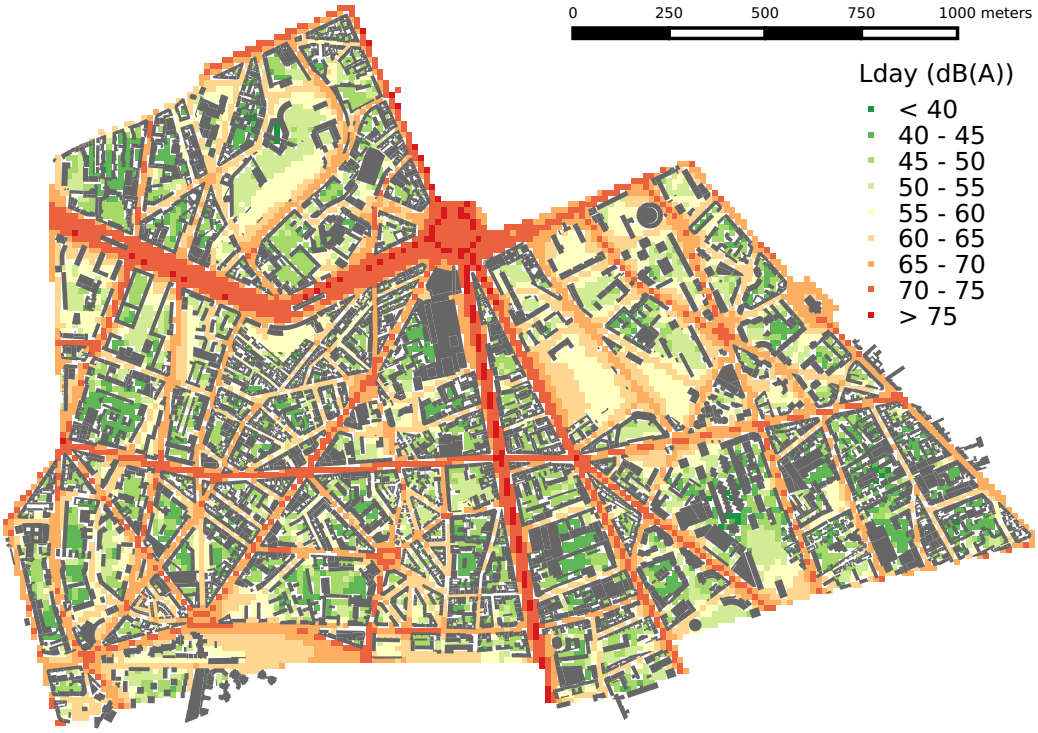

Figure 2: L_{day} level distribution over the study area

(between 06:00 and 18:00, local time), the evening (between 18:00 and 22:00) and the night (between 22:00 and 06:00) computed for the year 2014. These data are respectively given by the IGN , the French national geographical institute, and the city of Paris. Data like ground surface or altitude have been ignored in this study.

2.3.3. Real-time 1 h traffic and weather data

The real-time 1 h traffic data on the main roadways of Paris during the case study time period is available online on the city of Paris open data platform. For every measured track section, at every hour, the hourly average flow $F(t)$ (vehicles/h) and the occupation rate $R(t)$ (ratio of time during which the sensors detect an occupation) are given. Given the track section length ℓ_t and assuming an average vehicle length of $\ell_v = 4\,\mathrm{m}$, it is possible to estimate the average vehicle speed $S(t)$ on the track section in $\mathrm{km} \cdot \mathrm{h}^{-1}$:

$$S(t) = 3.6 \cdot \frac{F(t) \cdot \ell_v}{R(t) \cdot \ell_t} \tag{1}$$

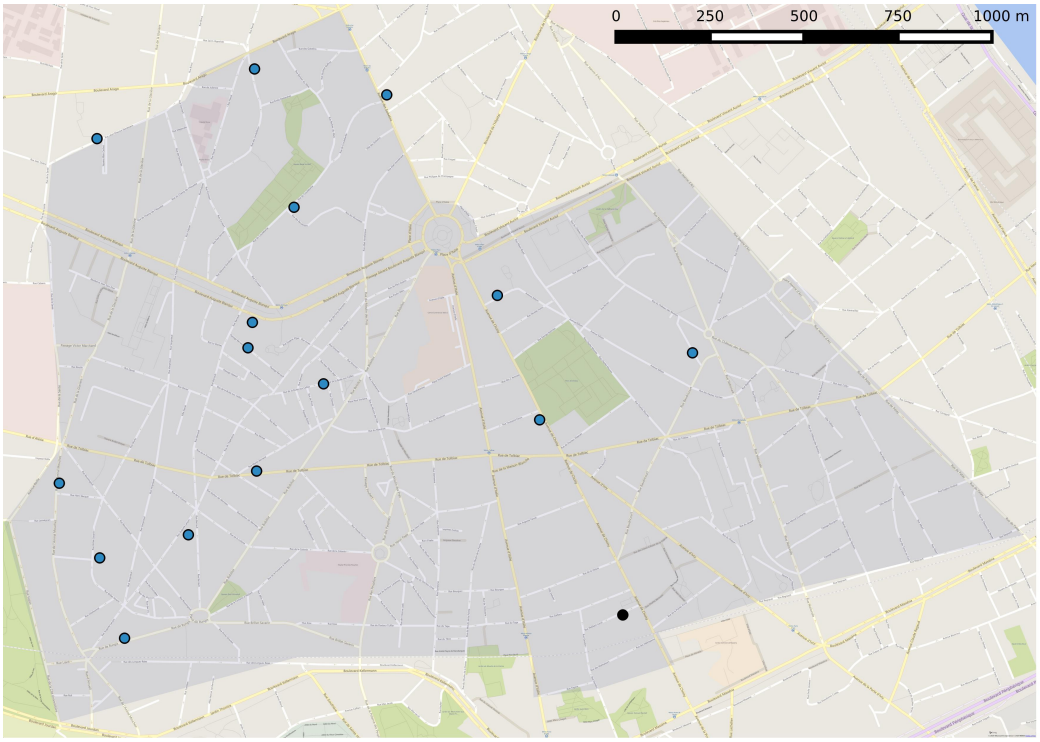

Figure 3: Distribution of the sensors across the study area, the observation point colored in black is the one which is displayed in figure 4

The real-time weather data has been taken from an open access source at the Montsouris weather station near the study area. The weather station updates its data every hour in real time. The reference noise mapping software only takes into account the temperature but upcoming versions might also take into account the wind intensity and direction, the temperature gradient, and more generally, the probability of occurrence of favourable atmospheric conditions.

2.4. Meta-model

This section introduces the tools built during the study and their justification: the meta-model and the design of its parameters (2.4.4).

2.4.1. Construction of the meta-model

When a noise map is computed with annually averaged input data, one may wonder how this noise map changes with a slight modification of the

parameters, e.g, a multiplicative coefficient applied to the traffic flow or a temperature variation in °C.

$\mathbf{p} \in \mathbb{R}^k$ denotes the input vector of parameters and $\mathcal{M}(\mathbf{p}) \in \mathbb{R}^n$ is the output of the reference noise mapping software. In order to speed up the computation of the hourly maps, a meta-model $\widehat{\mathcal{M}}(\mathbf{p})$ which is very similar to $\mathcal{M}(\mathbf{p})$ but with a computational time much lower (in this case, $\sim 100\,\text{ms}$ versus $\sim 1\,\text{h}$) is built. $\widehat{\mathcal{M}}$ is generated using a training sample of size $r = 2{\cdot}10^3$, $\{\mathbf{p}^{(1)}, \cdots, \mathbf{p}^{(r)}\}$ and the corresponding simulations $\{\mathcal{M}(\mathbf{p}^{(1)}), \cdots, \mathcal{M}(\mathbf{p}^{(r)})\}$. $\widehat{\mathcal{M}}$ is a weighted sum of a small number of maps obtained with a dimension reduction algorithm described in section 2.4.2, the weights are computed by a kriging interpolation function based on the weights of the training set described in section 2.4.3.

2.4.2. Dimension reduction

A PCA (Principal Components Analysis) (Jolliffe, 1986) algorithm determines which of the principal components explain most of the variance for the training sample. The structure of the noise mapping behavior allows us to explain more than 97 % of the variance with a short sequence of vectors $\{\mathbf{map}_i\}_{i\in[\![1,k]\!]}$ ($k \simeq 3$) as previously shown in (Lesieur et al., 2020):

$$\mathcal{M}(\mathbf{p}) = \bar{\mathbf{x}}_b + \sum_{i=1}^{k} w_i(\mathbf{p}) \times \boldsymbol{map}_i + \boldsymbol{\epsilon}, \tag{2}$$

where $\bar{\mathbf{x}}$ is the average of the training set outputs:

$$\bar{\mathbf{x}}_b = \frac{1}{r} \sum_{i=1}^{r} \mathcal{M}(\mathbf{p}^{(i)}), \tag{3}$$

$w_i(\mathbf{p})$ is the projection coefficient of the centered $\mathcal{M}(\mathbf{p})$ on $\boldsymbol{map}_i$,

$\boldsymbol{map}_i^T(\mathcal{M}(\mathbf{p}) - \bar{\mathbf{x}}_b)$, and $\boldsymbol{\epsilon}$ is the residual error.

2.4.3. Kriging

The reader might be familiar with kriging in its classical geostatistical background as it has been applied in some studies (Baume et al., 2009). However, contrary to the usual kriging employed in several acoustics applications using geographical data, this paper applies kriging to the abstract vector space of the input parameters which has no relation with the geographical 2D space.

The goal of the second step is to obtain for each map i selected in section 2.4.2 a fast approximation of the weight function:

$$\begin{array}{rccc} w_i & : & \mathbb{R}^k & \rightarrow & \mathbb{R} \\ & & \mathbf{p} & \mapsto & w_i(\mathbf{p}) \end{array} \tag{4}$$

where $w_i(\mathbf{p}^{(j)})$ is known for every $\mathbf{p}^{(j)}$ in the training sample. Kriging (Matheron, 1962) is a technique which allows to determine an approximation $\widehat{w}_i(\mathbf{p})$ of $w_i(\mathbf{p})$ by interpolating from the known values $w_i(\mathbf{p}^{(j)})$.

Once the kriging interpolators are computed for every projection vector, the meta-model $\widehat{\mathcal{M}}$ is defined as follows:

$$\widehat{\mathcal{M}}(\mathbf{p}) = \bar{\mathbf{x}}_b + \sum_{i=1}^{k} \widehat{w}_i(\mathbf{p}) \times \boldsymbol{map}_i \tag{5}$$

$\widehat{\mathcal{M}}(\mathbf{p})$ is a short sequence of elementary operations, hence its computation is much lower than the reference noise mapping software and then allows:

- A fast real-time computation of a noise map with the real-time input data;
- The generation of the statistical error covariance matrix $\mathbf{B}_{stat}$ with a Monte Carlo method, which will be used in data assimilation (See 2.5.2).

2.4.4. Design of the parameters

The parameters selected as inputs of the meta-model are shown in Table 1 with their respective amplitudes. For each input, the amplitude corresponds to the range of values observed in real-time.

Table 1: Input parameters and their input ranges for the meta-model. They are all dimensionless multiplicative coefficients applied to the reference values (the annually averaged daily values) except the temperature which is the actual value in °C.

Parameter	Minimum value	Maximum value
Light vehicle speed	0.1	2
Heavy vehicle speed	0.1	2
Light vehicle flow	0.1	2
Heavy vehicle flow	0.1	2
Temperature (°C)	-5	30

The goal of this section is to infer a value for the input coefficient from the real-time traffic data. As seen in the beginning of section 2.4.1, the input which represents traffic variations in the meta-model is a multiplicative coefficient applied to the annually averaged traffic data. It therefore models the variation in time of the traffic, and assumes a constant spatial distribution. Regarding the flow rate and the speed, the input data p_i is the ratio between the average quantity on the observed roads at a given time and the average quantity on the observed roads over one year.

Since the observed traffic data do not discriminate the heavy vehicles from the light vehicles, the same coefficient is applied to the heavy and light vehicle input — in other words, the fraction of heavy vehicle is assumed to be constant.

Figure 4 compares the time evolution of the measured noise level at an observation point and the corresponding output value of the meta-model with the input parameters built from the traffic and weather data. It shows that the meta-model fairly reproduces the hourly noise level distribution.

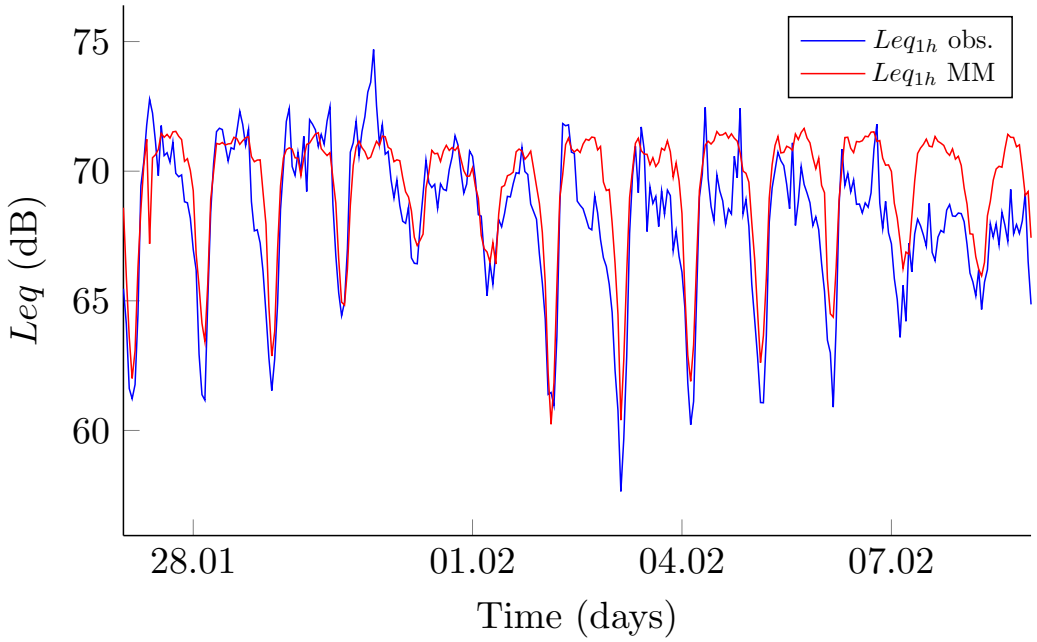

Figure 4: time evolution of the observed $LA_{eq,1h}$ and the meta-model output for the sensor point colored in black in figure 3

2.5. Data assimilation

2.5.1. Presentation

The data assimilation algorithm which will be used in this paper is called BLUE, for Best Linear Unbiased Estimator (Bouttier and Courtier, 2002). It makes use of the output of the meta-model and applies a correction which depends on $\mathbf{B}$, the covariance matrix of the simulation error, $\mathbf{R}$, the covariance matrix of the observational error, and the discrepancy between observations and simulations at the observation location. Matrices $\mathbf{B}$ and $\mathbf{R}$ characterize the spatial behavior of the model error and the observation error respectively.

At each timestep, a nominal noise map $\mathbf{x}^b = \widehat{\mathcal{M}}(\mathbf{p})$ is computed. It is an estimation of the real, exact state noise level distribution field $\mathbf{x}^t$. It is impossible to know the exact vector $\mathbf{x}^t$, either from the erroneous simulation or the incomplete (and slightly erroneous) observations. It would be the noise level field observed if each receiver had an ideal microphone on it. The set of observations is denoted $\mathbf{y} \in \mathbb{R}^p$. Let:

- $\mathbf{H} \in \mathbb{R}^{p \times n}$ be the observation matrix which maps a state vector, e.g., $\mathbf{x}^t$, to the observed values $\mathbf{y}$, so that $\mathbf{y}$ can be compared to $\mathbf{H}\mathbf{x}^t$. In this case, each observation point has a simulated counterpart, $\mathbf{H}$ is therefore a matrix in which each row is full of zeros except for a one in the column that corresponds to the receiver located at the observation point. The elements $[\mathbf{H}]_{ij}$ are equal to one if and only if the jth receiver corresponds to the ith observation point;
- $\mathbf{e}^b \in \mathbb{R}^n$ be the simulation error $\mathbf{x}^b - \mathbf{x}^t$, a random vector, which is assumed to be unbiased $\mathbb{E}[\mathbf{e}^b] = 0$;
- $\mathbf{e}^o \in \mathbb{R}^p$ be the observation error $\mathbf{y} - \mathbf{H}\mathbf{x}^t$, a random vector, which is assumed to be unbiased $\mathbb{E}[\mathbf{e}^o] = 0$;
- $\mathbf{B} = \mathbb{E}[\mathbf{e}^b \mathbf{e}^{bT}] \in \mathbb{R}^{n \times n}$ be the covariance matrix of the simulation error,
- $\mathbf{R} = \mathbb{E}[\mathbf{e}^o \mathbf{e}^{oT}] \in \mathbb{R}^{p \times p}$ be the covariance matrix of the observation error.

Based on $\mathbf{x}^b, \mathbf{B}, \mathbf{y}, \mathbf{R}$ and $\mathbf{H}$, an analysis state vector $\mathbf{x}^a$ is computed as the "Best Linear Unbiased Estimator" which is linearly dependent on $\mathbf{x}^b$ and $\mathbf{y}$, has unbiased error $\mathbf{e}^a = \mathbf{x}^a - \mathbf{x}^t$, and has an error variance with minimum trace (Bouttier and Courtier, 2002). This estimator is uniquely defined as

follows, under the assumption that the simulation and observation errors are uncorrelated:

$$\mathbf{x}^a = \mathbf{x}^b + \mathbf{K}(\mathbf{y} - \mathbf{H}\mathbf{x}^b) \tag{6}$$

where

$$\mathbf{K} = \mathbf{B}\mathbf{H}^T(\mathbf{H}\mathbf{B}\mathbf{H}^T + \mathbf{R})^{-1} \tag{7}$$

$\mathbf{K}$ is called the gain matrix or the Kalman matrix. The observation errors at two different receivers are not correlated. The observation error essentially depends on the accuracy of the microphone which is described by its standard deviation σ_r, therefore:

$$\mathbf{R} = \sigma_r^2 \mathbf{I}_p \tag{8}$$

with $\mathbf{I}_p$ the identity matrix of dimension p. In the rest of the study, σ_r =1 dB^2, which corresponds to the industrial accuracy of the sensor.

2.5.2. Computation of the simulation error covariance matrix $\mathbf{B}$

A good estimation of the covariance matrix $\mathbf{B}$ is crucial to perform an efficient data assimilation. There are two approaches to compute the simulation error covariance matrix: analytical and statistical. On the one hand, the analytical approach gives a covariance formula based on the assumption that where there is an error on the noise estimation at a given location, the traffic estimation is subject to similar errors in the surrounding streets. On the other hand, the statistical approach generates an error covariance matrix between the meta-model output and the ideal meta-model output, with a large random selection of noise maps made possible by the short computation time of the meta-model in a Monte Carlo algorithm.

Analytical covariance matrix $\mathbf{B}_{ana}$. A parametrized simulation error covariance function has been successfully used in a previous work (Ventura et al., 2018). The simulation error cross correlations between two receivers i and j are expressed in terms of:

- d_{ij}, the length of the shortest path along the road network between the projection of receivers i and j on the closest road computed with a Johnson algorithm (Johnson, 1977) and shown for a specific observation point in figure 5,
- the nominal noise field itself, through a correlation function $\rho(x_i, x_j)$, where x_i and x_j are the values of $\mathbf{x}^b$ at points i and j as proposed by

(Riishøjgaard, 2002). The corresponding simulation error covariance between points i and j reads:

$$[\mathbf{B}_{ana}]_{ij} = \sigma_b^2 \exp\left(-\frac{d_{ij}}{L_d}\right) \exp\left(-\frac{|x_i - x_j|}{L_b}\right) \tag{9}$$

where σ_b^2 is the characteristic variance of each point, L_d is a characteristic distance in m and L_b is a characteristic noise level value in dB.

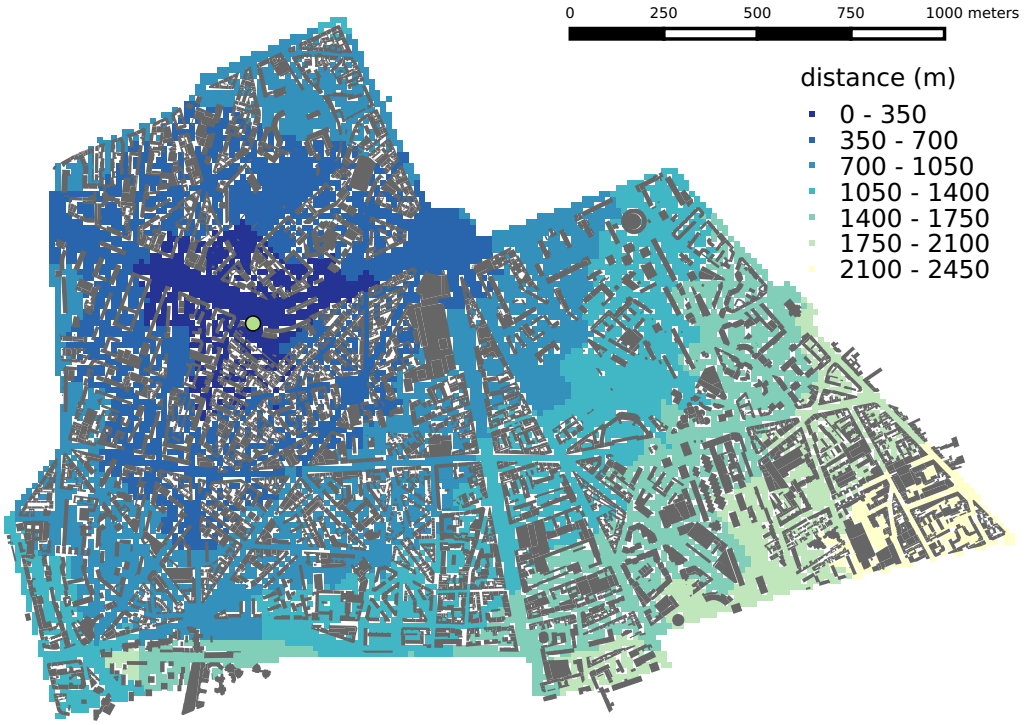

Figure 5: This map displays the distance along the road network between the highlighted point and the other points of the simulated map

Figure 6 shows the covariance between the same specific point and the other points, using the analytic covariance function with $\sigma_b^2 = 67\,\mathrm{dB}^2(\mathrm{A})$, $L_d = 500\,\mathrm{m}$ and $L_b = 6\,\mathrm{dB}$ ($A = 1.03$). These values were validated by a method called χ^2 diagnosis which checks whether the observations are consistent with the formulation of their error covariance (see appendix for further details). These values are consistent with other studies that computed the correlation length of the noise error distribution such as (Aumond et al.,

2018). It points out that the correlation is mostly significant for the points located in the neighborhood of the selected point.

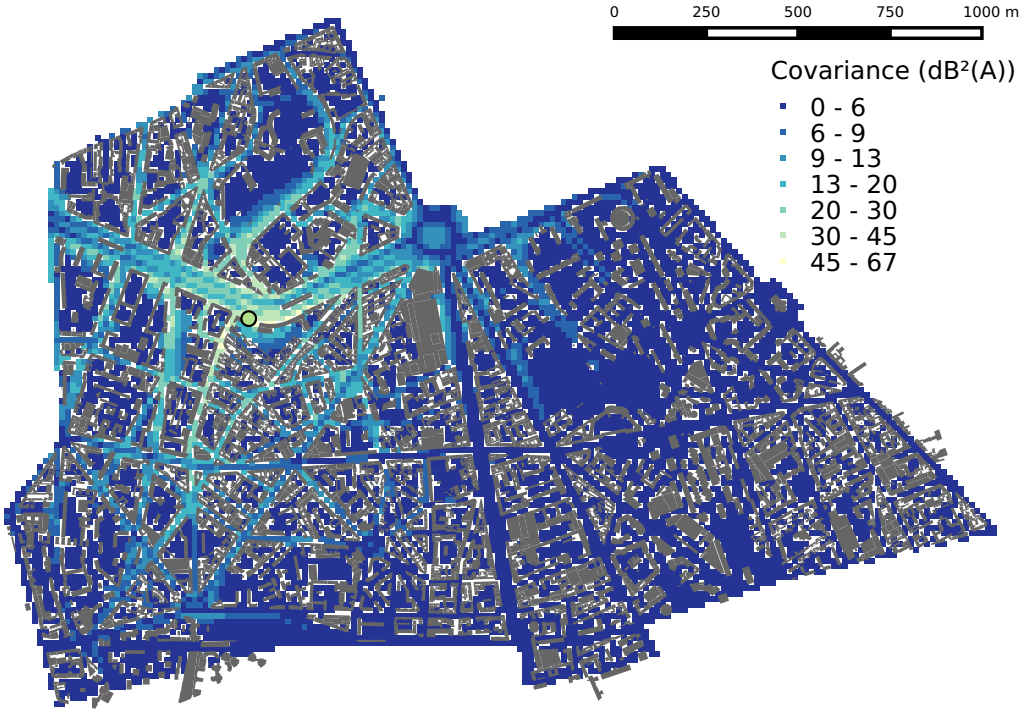

Figure 6: This map displays the analytical covariance between the highlighted point and the other points of the simulated map

Statistical covariance matrix $\mathbf{B}_{stat}$. The meta-model allows to run a large number of simulations. It is possible to compute the error covariance matrix between the simulated noise map and the ideal meta-model output, within the subspace $\{\boldsymbol{map}_i\}_i$ of the meta-model $\mathbf{B}_{stat}$ with a Monte Carlo algorithm (Fishman, 1996), sampling the uncertainties. Let $\{\mathbf{p}^{(1)}, \cdots, \mathbf{p}^{(N)}\}$ be N random draws of a uniform distribution over the input interval (in this case study, $N = 3{\cdot}10^4$). Then, with:

$$\bar{\mathbf{x}}^b = \frac{1}{N} \sum_{k=1}^{N} \widehat{\mathcal{M}}(\mathbf{p}^{(k)}) \tag{10}$$

$\mathbf{B}_{stat}$ is defined by:

$$\mathbf{B}_{stat} = \frac{1}{N-1} \sum_{k=1}^{N} \left(\widehat{\mathcal{M}}(\mathbf{p}^{(k)}) - \bar{\mathbf{x}}^b \right) \left(\widehat{\mathcal{M}}(\mathbf{p}^{(k)}) - \bar{\mathbf{x}}^b \right)^T \tag{11}$$

Figure 7 shows, for the same point as in figure 6, the covariance function computed with the Monte Carlo algorithm. Since the dimension of the subspace is very low, it has a much more global distribution, the low ranking implies that an error covariance at some receiver is likely to be correlated with an error covariance of any receiver elsewhere in the study area. The point is not only correlated to its neighborhood but with all the points of the map located near a roadway.

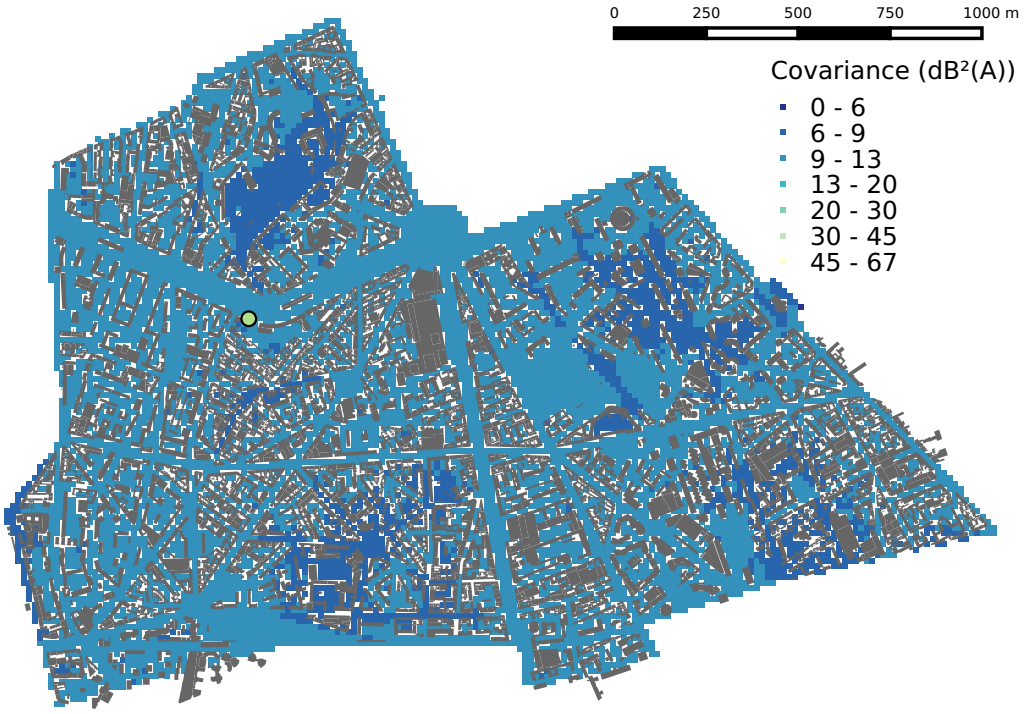

Figure 7: This map displays the statistical covariance of each point with the highlighted point

Sum of the analytical and statistical covariance matrices. The covariance matrix $\mathbf{B}_{ana}$ built as in section 2.5.2 has shown good results in studies where

the data assimilation is computed on one fixed nominal noise map (Ventura et al., 2018). On the other hand, the statistical matrix $\mathbf{B}_{stat}$ cannot be used alone for data assimilation since it only applies on the reduced subspace and thus cannot be used to compute the covariance of $\mathbf{x}^b - \mathbf{x}^t$. In the appendix, the authors have shown that a good error covariance matrix for a data assimilation process, performed on a noise map generated with a meta-model, is the sum of the two previous covariance matrices: $\mathbf{B}_{ana} + \mathbf{B}_{stat}$.

2.6. Validation method

The leave-one-out cross-validation consists in removing the observations of a given microphone from the data assimilation process. Only the observations from the other microphones are used to correct the noise level map. This procedure is carried out for all microphones, one by one — only one microphone is removed at a time. At the location of the removed microphone, the meta-model performance is compared to the performance after assimilation of the observations of the other microphones. This allows to check whether the assimilation properly propagates in space the corrections that originate from the observed locations. The cross-validation evaluates the effects of the data assimilation at locations without any observations.

The bias and RMSE indicators defined in table 2 are used to quantify the performance of the simulations for the $LAeq_{1h}$.

Table 2: Scores for the performance evaluation of a model. $(c_i)_i$ is the simulated sample. $(o_i)_i$ is the corresponding observed sample. n is the total number of elements in the sample. $\bar{c}$ and $\bar{o}$ are respectively the mean of $(c_i)_i$ and $(o_i)_i$. RMSE stands for Root Mean Square Error.

Score	Formula
Bias	$\frac{1}{n}\sum_{i=1}^{n}(c_i - o_i)$
RMSE	$\sqrt{\frac{1}{n}\sum_{i=1}^{n}(c_i - o_i)^2}$

3. Results

3.1. Cross validation

3.1.1. Dispersion

Figure 8 shows the error dispersion for all the indicators at every step of the data assimilation process (meta-modeling, data assimilation with $\mathbf{B} = \mathbf{B}_{ana}$, data assimilation with $\mathbf{B} = \mathbf{B}_{ana} + \mathbf{B}_{stat}$). The distribution gets narrower as the precision of the data assimilation process increases. This evolution is also presented in table 3 where the evolution of the absolute bias is showed at each level of correction.

Table 3: Dispersion in dB(A) of the error between the observation and the simulation or the analysis in leave-on-out cross-validation for all the microphones during all the measurement campaign

error amplitude (dB)	$[0, 1]$	$[1, 3]$	$[3, 5]$	> 5
meta-model	18 %	33 %	26 %	22 %
assimilation with $\mathbf{B} = \mathbf{B}_{ana}$	26 %	41 %	22 %	10 %
assimilation with $\mathbf{B} = \mathbf{B}_{ana} + \mathbf{B}_{stat}$	30 %	44 %	18 %	8 %

In addition, Figure 9 shows the time evolution of the observed and assimilated sound levels at the same reception point and during the same time period as in figure 4. The temporal evolution of sound levels is finely reproduced by the data assimilation process.

3.1.2. RMSE

The root mean squared error of the $LA_{eq,1h}$ is displayed for each month in figure 10 at every step of the data assimilation process. The reduction of the error covariance is noticeable. At each step, the RMSE is reduced and goes down to an average of 2.9 dB(A) at the final stage.

As expected in section 2.5.2, the matrix $\mathbf{B} = \mathbf{B}_{ana} + \mathbf{B}_{stat}$ better characterize the error covariance behavior and gives better results than $\mathbf{B}_{ana}$ alone for both dispersion and RMSE.

3.1.3. Distance to the network

This section proposes to connect the individual performance of the receiver with its position in the road network. Table 4 shows the performance of the data assimilation process at each receiver.

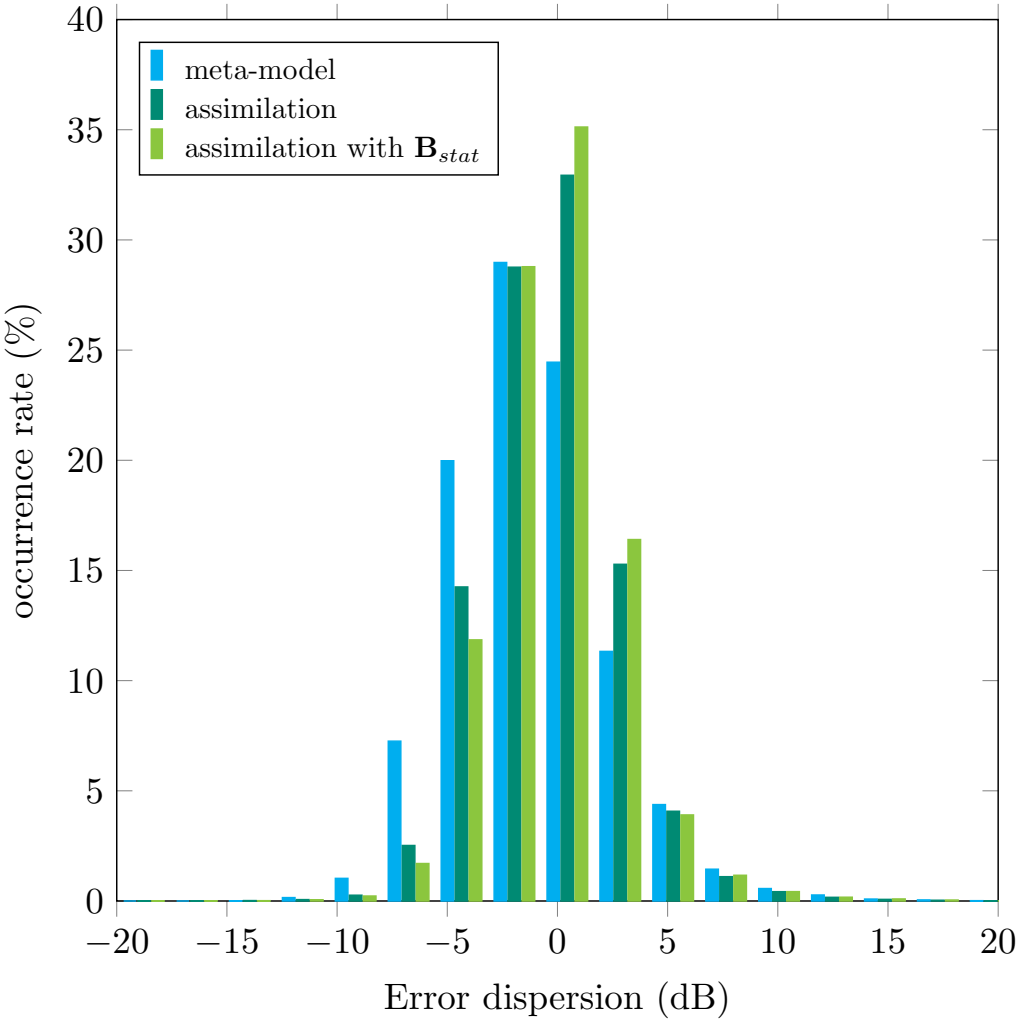

Figure 8: Dispersion in dB(A) of the error between the observation and the simulation (blue) or the assimilation in leave-on-out cross-validation (green) for all the microphones during all the measurement campaign.

Figure 11 shows the RMSE reduction percentage ρ (equation (12)) in the leave-one-out cross validation context with respect to the distance of the observation point to the network (i.e., the distance to the nearest microphone).

$$\rho = 100 \cdot \frac{\mathrm{RMSE}_{meta-model} - \mathrm{RMSE}_{assimilation}}{\mathrm{RMSE}_{assimilation}} \tag{12}$$

The dependency on the distance to the network is mainly unnoticeable.

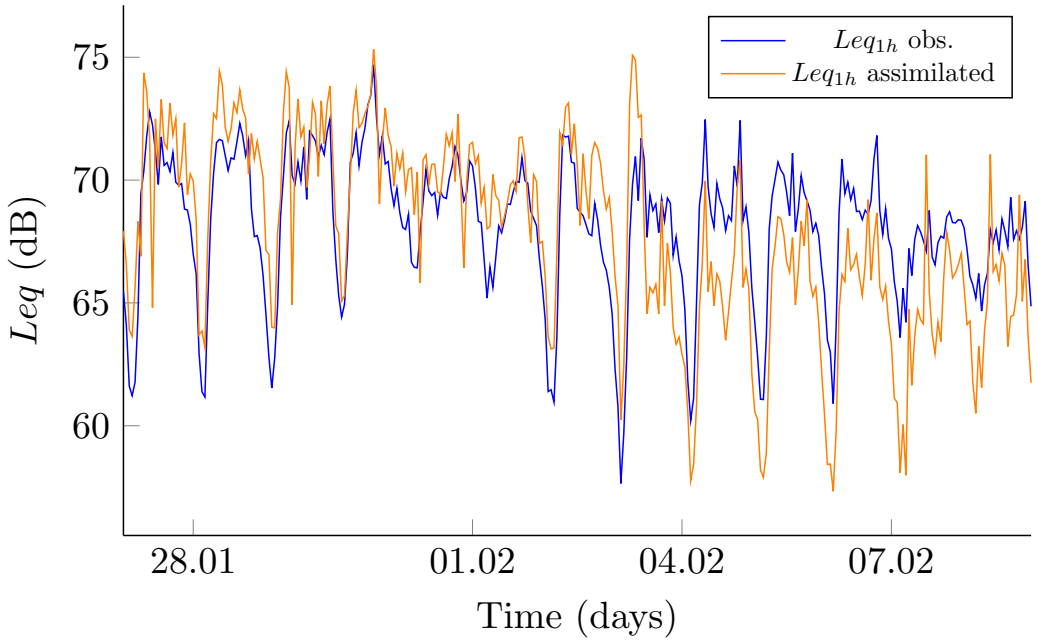

Figure 9: time evolution of the observed $LA_{eq,1h}$ and the leave-one-out data assimilation process output for the sensor point colored in black in figure 3

This is explained by the distribution of the Monte Carlo covariance matrix which is mainly non-local. The RMSE reduction shows that an error covariance between two points of the network depends on other factors than the distance between them or the difference between their noise levels. Some future studies shall work on identifying these factors, such as for instance, the nature of the roads linked to the receivers.

3.2. Spatial analysis

Figure 12 shows how the correction due to the observations propagates across the study area when $\mathbf{B} = \mathbf{B}_{ana} + \mathbf{B}_{stat}$. It follows the intuition that for every observation point, the correction its neighborhood receives grows with the underestimation of its sound level.

4. Discussion

The global RMSE reduction of all the points is noticeable and proves the efficiency of this approach. Since $\mathbf{B}$ has been built partly under the assumption that the noise errors are correlated along the road network, the data

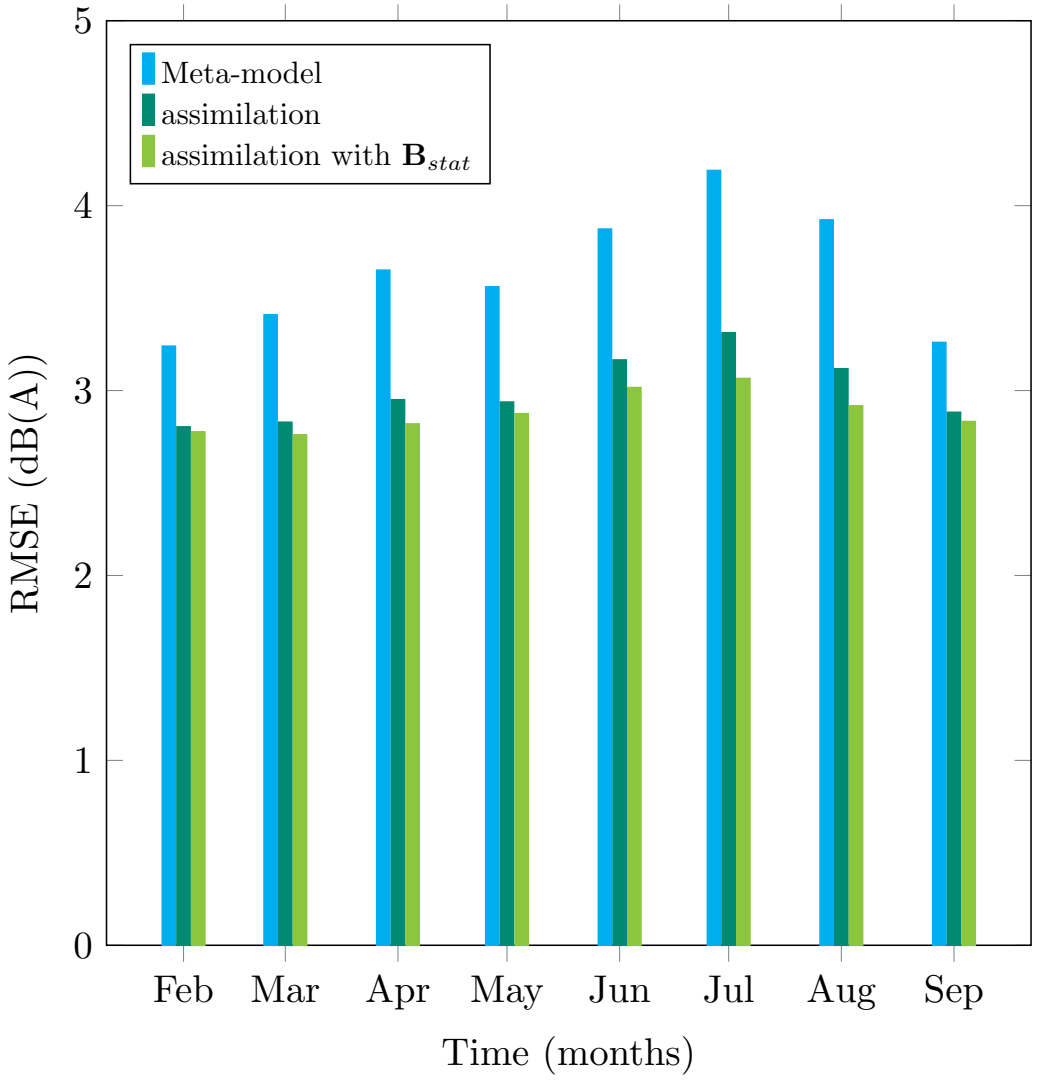

Figure 10: RMSE in dB(A) of the error between the observation and the nominal noise level values (blue) or the analysis in leave-on-out cross-validation (green) for all the microphones, for each month of the measurement campaign. It is noticeable to observe that the summer months have a higher error rate, which is strongly corrected by the data assimilation.

assimilation procedure shall apply in so far as the traffic is the predominant source of noise pollution at the observation points, and the bias remains low.

Amongst all the parameters shown in table 1, the parameter "wall absorp-

Table 4: Performance of the noise map and computed with the meta-model and the assimilation regarding the observations at each microphone point, the values are given in dB(A)

Node	Bias meta-model	Bias assimilation	RMSE
251	-2.19	-0.16	1.97
252	-3.41	-1.79	3.72
254	-0.12	0.13	2.20
255	0.88	0.92	2.65
256	0.42	0.86	2.28
259	1.72	1.42	3.71
261	-2.65	-1.30	3.07
262	-0.37	0.67	2.07
264	3.00	0.93	3.17
265	1.71	0.72	3.22
266	-2.02	-0.59	1.75
268	-5.22	-2.31	4.08
270	-2.93	-0.46	1.87
272	-2.81	-1.04	2.62
274	-4.35	-1.60	2.90
275	-0.35	-0.05	3.25

tion coefficient" is not taken into account in the data assimilation process. It has in fact been set to 0.2 during the whole study. Another value would give better results on some areas of the case study and worse results on others, since there is a variability of the absorption coefficient along the buildings. The meta-model has been built this way for other analyses such as sensitivity analysis or inverse modeling, where more parameters are necessary in the meta-model than the condition parameters (Le Gratiet et al., 2017).

The number of parameters chosen for this study is restricted, some meta-models segregate road categories into minor, medium and major roads due to their different traffic dynamics (Barrigón Morillas et al., 2005). With a finer granularity, it is possible to better seize the noise dynamics. However, in this study, the lack of traffic data out of the major axes will preclude achieving higher levels of precision.

The observational data in this study have not been specifically collected for data assimilation purposes. An interesting approach would be to explore how the spatial distribution and the number of receivers affect the results

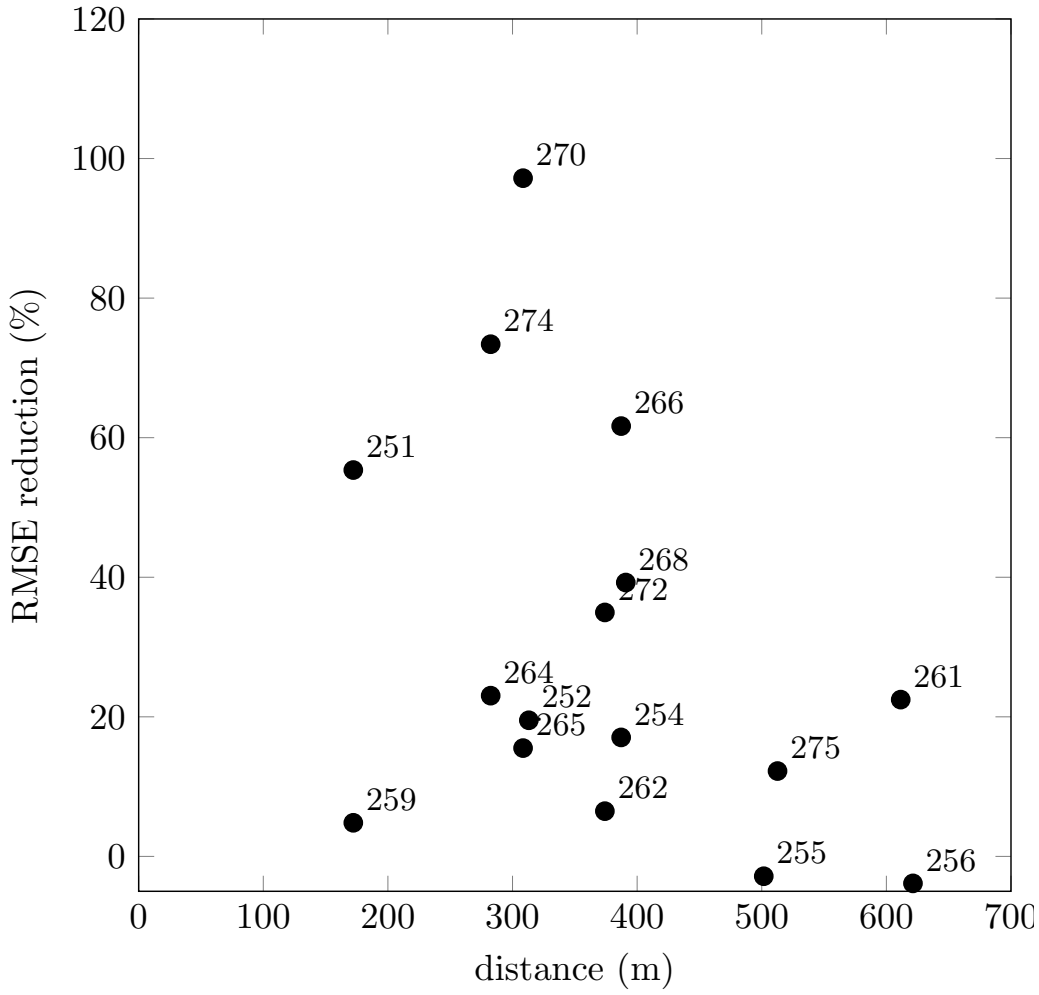

Figure 11: RMSE reduction rate versus the distance to the network for data assimilation with the statistical covariance matrix $\mathbf{B}_{stat}$

of the data assimilation procedure. The CENSE project aims to study this question by displaying a large amount of microphones across a study area in order to optimize the data assimilation reference procedure for model and observation-based noise mapping design.

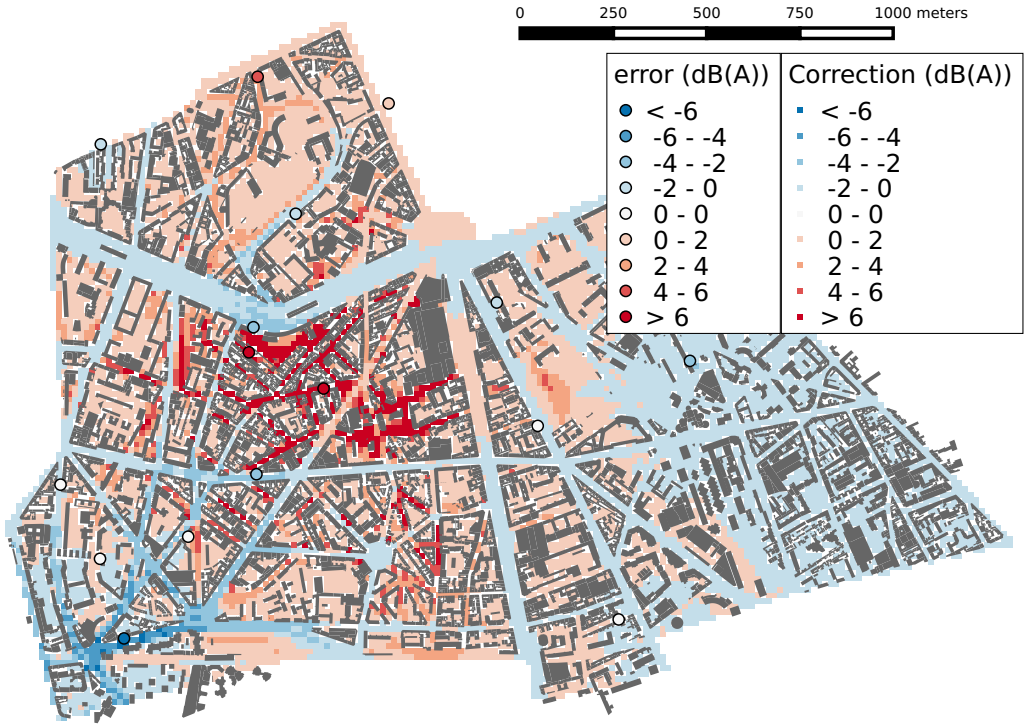

Figure 12: This map displays an example of the correction induced by the assimilation of the observations at a given time. The error disks are the $\mathbf{e}^b$ at the observation points, and the map represents the data assimilation correction over the map. The chosen date is June, 21 at 22:00, during a popular music festival (fête de la musique), hence the observation error and the correction are rather high. The positively corrected area is a lively neighborhood with a high density of bars and restaurants (Butte-aux-Cailles).

5. Conclusion

The data assimilation applied to noise maps generated through a meta-model improves the performance of the generated noise map, from an average RMSE of 3.9 dB(A) to 2.8 dB(A), and better grasps the hourly evolution of the noise level distribution across the study area than a meta-model alone.

The process was carried out in three steps, the collection of data for the road traffic, the generation of the meta-model (section 2.4.1), and then the data assimilation itself (section 2.5.1)

This gain matrix $\mathbf{K}$ has been computed with the simulation error covariance matrix $\mathbf{B}$ and the observation error covariance matrix $\mathbf{R}$. $\mathbf{B}$ is the sum of two matrices $\mathbf{B}_{stat}$ and $\mathbf{B}_{ana}$.

- On the one hand, $\mathbf{B}_{ana}$ is called the analytical covariance matrix and relies on a simulation error propagation analytical model whose parameters have been designed with a so-called χ^2 diagnosis (section 2.5.2). It takes into account the physical behavior of a simulation error on a road network.

- On the other hand, $\mathbf{B}_{stat}$ has been statistically generated with a large number of calls to the meta-model using a Monte Carlo algorithm (section 2.5.2). It describes the behavior of the error between the meta-model output given by the traffic and weather observations and the ideal meta-model output.

New data assimilation techniques relying on a meta-model are yet to be explored. The first among them is inverse modeling which aims at approaching the true input parameters of the meta-model with the help of the noise observations. This method requires an enrichment of the meta-model with more uncertain input data (height of the building, ground absorption, topography uncertainty, etc.) in order to increase the number of degrees of freedom. The distribution of the sensors across the network also needs to be optimized, and further investigation will be dedicated to the optimization of the network of sensors.

Acknowledgments

The authors would like to thank the CENSE project (ref. ANR-16-CE22-0012) team for initiating this project, the Agence Nationale de la Recherche (ANR) for their financial support, the city of Paris and BRUITPARIF for granting access to their data, GRAFIC project for the measurement campaign whose noise data were used for the data assimilation and Nicolas Fortin of the UMRAE department at Université Gustave Eiffel for his technical support on the NoiseModelling software. The authors would also like to express their grateful aknowledgements to Dr. Isaac Jones and Dr. Ian Jones for their careful reading of the article which has greatly improved it.

Aumond, P., Can, A., Mallet, V., De Coensel, B., Ribeiro, C., Botteldooren, D., Lavandier, C., 2018. Kriging-based spatial interpolation from measurements for sound level mapping in urban areas. The Journal of the Acoustical Society of America 143, 2847–2857. URL: https://doi.org/10.1121/1.5034799, doi:10.1121/1.5034799.

Aumond, P., Fortin, N., Can, A., 2020. Overview of the noisemodelling open-source software version 3 and its applications, in: Proceedings of the 49th International Congress and Exhibition on Noise Control Engineering e-congress, p. 0.

Barrigón Morillas, J.M., Escobar, V., Sierra, J.A., Vílchez-Gómez, R., Vaquero, J., Trujillo Carmona, J., 2005. A categorization method applied to the study of urban road traffic noise. The Journal of the Acoustical Society of America 117, 2844–52. doi:10.1121/1.1889437.

Baume, O., Gauvreau, B., Berengier, M., Junker, F., Wackernagel, H., Chiles, J.P., 2009. Geostatistical modeling of sound propagation: Principles and a field application experiment. The Journal of the Acoustical Society of America 126, 2894–904. doi:10.1121/1.3243301.

Bocher, E., Guillaume, G., Picaut, J., Petit, G., Fortin, N., 2019. Noisemodelling: An open source gis based tool to produce environmental noise maps. ISPRS International Journal of Geo-Information 8. URL: https://www.mdpi.com/2220-9964/8/3/130, doi:10.3390/ijgi8030130.

Bouttier, F., Courtier, P., 2002. Meteorological Training Course Lecture Series. ECMWF. chapter Data Assimilation Concepts and Methods. p. 0. URL: https://www.ecmwf.int/node/16928. learning.

De Coensel, B., Sun, K., Wei, W., Van Renterghem, T., Sineau, M., Ribeiro, C., Can, A., Aumond, P., Lavandier, C., Botteldooren, D., 2015. Dynamic noise mapping based on fixed and mobile sound measurements, in: Proceedings of the 10th European Congress and Exposition on Noise Control Engineering, pp. 2339–2344.

Eerden, F., Graafland, F., Wessels, P., Segers, A., Salomons, E., 2014. Internoise 2014 - 43rd international congress on noise control engineering: Improving the world through noise control, in: Model based monitoring of traffic noise in an urban district, p. 0.

European Commission, 2015. Commission directive (eu) 2015/996 of 19 may 2015 establishing common noise assessment methods according to directive 2002/49/ec of the european parliament and of the council (text with eea relevance). URL: http://data.europa.eu/eli/dir/2015/996/oj.

Fishman, G.S., 1996. Monte Carlo: Concepts, Algorithms and Applications. Springer Verlag, New York, NY, USA.

Johnson, D.B., 1977. Efficient algorithms for shortest paths in sparse networks. J. ACM 24, 1–13. URL: http://doi.acm.org/10.1145/321992.321993, doi:10.1145/321992.321993.

Jolliffe, I., 1986. Principal Component Analysis. Springer Verlag.

Kephalopoulos, S., PAVIOTTI, M., Anfosso-Lédée, F., 2012. Common noise assessment methods in Europe (CNOSSOS-EU). PUBLICATIONS OFFICE OF THE EUROPEAN UNION. URL: https://hal.archives-ouvertes.fr/hal-00985998, doi:10.2788/31776.

Lavandier, C., Aumond, P., Gomez, S., Domingus, C., 2016. Urban soundscape maps modelled with geo-referenced data. Noise Mapping 3. doi:10.1515/noise-2016-0020.

Le Gratiet, L., Marelli, S., Sudret, B., 2017. Metamodel-Based Sensitivity Analysis: Polynomial Chaos Expansions and Gaussian Processes. Springer International Publishing, Cham. chapter 1. pp. 1289–1325. URL: https://doi.org/10.1007/978-3-319-12385-1, doi:10.1007/978-3-319-12385-1.

Lesieur, A., Aumond, P., Mallet, V., Can, A., 2020. Meta-modeling for urban noise mapping. The Journal of the Acoustical Society of America 148, 3671–3681. URL: https://doi.org/10.1121/10.0002866, doi:10.1121/10.0002866, arXiv:https://doi.org/10.1121/10.0002866.

Matheron, G., 1962. Traité de géostatistique appliquée. 1 (1962). volume 1. Editions Technip.

Ménard, R., Cohn, S.E., Chang, L.P., Lyster, P.M., 2000. Assimilation of stratospheric chemical tracer observations using a kalman filter. part i: Formulat. Monthly Weather Review doi:10.1175/1520-0493(2000)128¡2654:AOSCTO¿2.0.CO;2.

Riishøjgaard, L., 2002. A direct way of specifying flow-dependent background error correlations for meteorological analysis systems. Tellus A 50, 42–57. doi:10.1034/j.1600-0870.1998.00004.x.

Tilloy, A., Mallet, V., Poulet, D., Pesin, C., Brocheton, F., 2013. Blue-based no 2 data assimilation at urban scale. Journal of Geophysical Research: Atmospheres 118. doi:10.1002/jgrd.50233.

Ventura, R., Mallet, V., Issarny, V., 2018. Assimilation of mobile phone measurements for noise mapping of a neighborhood. Journal of the Acoustical Society of America 144, 1279 – 1292. URL: `https://hal.inria.fr/hal-01909933`, doi:10.1121/1.5052173.

Wei, W., Van Renterghem, T., De Coensel, B., Botteldooren, D., 2016. Dynamic noise mapping: A map-based interpolation between noise measurements with high temporal resolution. Applied Acoustics 101, 127–140. doi:10.1016/j.apacoust.2015.08.005.

Zambon, G., Benocci, R., Bisceglie, A., Roman, H., Bellucci, P., 2016. The life dynamap project: Towards a procedure for dynamic noise mapping in urban areas. Applied Acoustics doi:10.1016/j.apacoust.2016.10.022.

Appendix A. $\boldsymbol{\chi^2}$ diagnosis

Appendix A.1. χ^2 diagnosis

With d_{ij} and $|x_i - x_j|$ known for all $(i,j) \in [\![1,n]\!]^2$, the characteristic values σ_b, L_d and L_b must be tuned to optimize the efficiency of the analytical covariance matrix.

To do so, a χ^2 diagnosis is carried out. It consists in checking the consistency between the available innovations $\boldsymbol{\nu}_t = \mathbf{y}_t - \mathbf{H}_t\mathbf{x}_t^b$ and their variances $\mathbf{S}_t = \mathbf{H}_t\mathbf{B}\mathbf{H}_t^T + \mathbf{R}_t$ for each time step t. This method has proved to be useful in the meteorology (Ménard et al., 2000) and in other fields. Let χ_t^2 be the scalar:

$$\chi_t^2 = \boldsymbol{\nu}_t^T \mathbf{S}_t^{-1} \boldsymbol{\nu}_t \tag{A.1}$$

Its expected value is

$$\begin{aligned}\mathbb{E}[\chi_t^2] &= \mathbb{E}[\boldsymbol{\nu}_t^T \mathbf{S}_t^{-1} \boldsymbol{\nu}_t] \\ &= \mathrm{tr}(\mathbf{S}_t^{-1} \mathbb{E}[\boldsymbol{\nu}\boldsymbol{\nu}^T]) \\ &= \mathrm{tr}(\mathbf{S}_t^{-1}\mathbf{S}_t) = \mathrm{tr}(\mathbf{I}_{p_t}) = p_t\end{aligned} \tag{A.2}$$

p_t being the dimension of $\mathbf{y}_t - \mathbf{H}_t\mathbf{x}_t^b$ at time t. The dimension of $\mathbf{y}_t$ may vary in time since the microphones may not be all simultaneously active, and so does $\mathbf{R}_t$, $\mathbf{H}_t$ and $\mathbf{S}_t$. Let A be the value:

$$A = \frac{1}{|\mathcal{T}|} \sum_{t \in \mathcal{T}} \frac{\chi_t^2}{p_t} \tag{A.3}$$

The parameters σ_b, L_d and L_b are chosen so that A is close to 1.

Appendix A.2. Note on the χ^2 diagnosis

According to the definition of section 2.5.2, the covariance matrix $\mathbf{B}_{ana}$ is no longer the simulation error covariance but the covariance of the vector $\boldsymbol{\Psi}^T\boldsymbol{\Psi}\mathbf{x}^t - \mathbf{x}^t$, with $\boldsymbol{\Psi}$ the matrix which concatenates the basis vector of the reduced subspace. Hence the characteristic parameters obtained with the χ^2 diagnosis are ill defined. However, since $\mathbf{x}^b$ remains a fairly good approximation of $\boldsymbol{\Psi}^T\boldsymbol{\Psi}\mathbf{x}^t$, the orders of magnitude of the characteristic parameters obtained with this method are still satisfying.

Appendix B. Sum of the analytical and statistical covariance matrices

By construction of the meta-model, $\mathbf{x}^b$ lies in the subspace generated by the maps set of the metamodel $\{\boldsymbol{map}_i\}_{i \in [\![1,k]\!]}$ with $k \ll n$. This suggests to decompose the observation in two orthogonal components $\widehat{\mathbf{e}}^b \in \mathrm{Im}(\boldsymbol{\Psi}^T\boldsymbol{\Psi})$ and $\widetilde{\mathbf{e}}^b \in \mathrm{Im}(\boldsymbol{\Psi}^T\boldsymbol{\Psi})^\perp$ as illustrated in figure B.13. The current section shows that the construction of $\mathbf{x}^b$ allows that a new covariance matrix $\mathbf{B}$ can be generated by adding the analytical covariance matrix defined in section 2.5.2 $\mathbf{B}_{ana}$ to a statistically defined covariance matrix $\mathbf{B}_{stat}$.

The simulation error can be decomposed as follows: $\mathbf{e}^b = \widehat{\mathbf{e}}^b + \widetilde{\mathbf{e}}^b$. $\widehat{\mathbf{e}}^b$ is the modeling error that grasps the error due to model approximations, and the discrepancy between the estimated input parameters and the true parameters. $\widetilde{\mathbf{e}}^b$ is the fluctuation error due to the noise level components which are

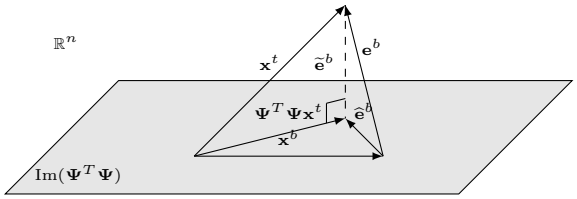

Figure B.13: Geometrical interpretation of the relation between the statistical and the analytical covariance matrices

not related to the traffic noise. Its covariance matrix is expressed with the analytical covariance matrix described in section 2.5.2. Under the assumption that these two components are independent ($\mathbb{E}[\widehat{\mathbf{e}}^b\widetilde{\mathbf{e}}^{bT}] = \mathbb{E}[\widetilde{\mathbf{e}}^b\widehat{\mathbf{e}}^{bT}] = 0$), $\mathbf{B}$ can be expressed as

$$\begin{aligned}\mathbf{B} = \mathbb{E}[\mathbf{e}^b{\mathbf{e}^b}^T] &= \mathbb{E}[(\widehat{\mathbf{e}}^b + \widetilde{\mathbf{e}}^b)(\widehat{\mathbf{e}}^b + \widetilde{\mathbf{e}}^b)^T] \\ &= \mathbb{E}[\widehat{\mathbf{e}}^b\widehat{\mathbf{e}}^{bT} + \widetilde{\mathbf{e}}^b\widetilde{\mathbf{e}}^{bT} + \widetilde{\mathbf{e}}^b\widehat{\mathbf{e}}^{bT} + \widehat{\mathbf{e}}^b\widetilde{\mathbf{e}}^{bT}] \\ &= \mathbf{B}_{stat} + \mathbf{B}_{ana} + \underbrace{\mathbb{E}[\widetilde{\mathbf{e}}^b\widehat{\mathbf{e}}^{bT} + \widehat{\mathbf{e}}^b\widetilde{\mathbf{e}}^{bT}]}_{=0} \\ &= \mathbf{B}_{stat} + \mathbf{B}_{ana}\end{aligned} \tag{B.1}$$

A way to check the validity of this assumption is to evaluate the norm of the projection $\Pi_{\mathrm{Im}(\mathbf{B}_{stat})}$ of the eigenvectors of $\mathbf{B}_{ana}$ onto $\mathrm{Im}(\mathbf{B}_{stat})$. In this case study, for each eigenvector $\boldsymbol{v}_i$ of $\mathbf{B}_{ana}$. The values remain low

$$\frac{\|\Pi_{\mathrm{Im}(\mathbf{B}_{stat})}(\boldsymbol{v}_i)\|}{\|\boldsymbol{v}_i\|} < 5\,\% \tag{B.2}$$